of the X_λ which are more general than (2) may be used. In the first place, although it is probably most convenient to use (5a) for the potential energy of u_p, it is not necessary to do so, and one may consider the use of an independent-particle potential energy which minimizes the spread W of the p-group strength functions. Secondly, it is apparent that, with the exception of (4) and (5), the formulas of II remain valid even if the ψ_c are allowed to depend parametrically on the coordinate $\mathbf{r}_n$ of the incident particle. Such a parametric dependence of ψ_c on $\mathbf{r}_n$ corresponds to a polarization of the residual nucleus[20] by the incident nucleon, and one may hope that the corresponding $\psi_c(\mathbf{r}_1,\mathbf{r}_2,\cdots\mathbf{r}_A;\mathbf{r}_n)u_p(\mathbf{r}_n)$ takes the interaction of the last nucleon with the residual nucleus more fully into account than the $\psi_c u_p$ of (2). As a result, the square integral of $(V-E_{cp})\psi_c u_p$ will become smaller and the calculated width of the giant resonance less than as given above. This second possibility would seem to contradict the calculations carried out above and are, in fact, compatible with them only if (8a) and (8b) are not valid. The explanation is that the terms of (7a) can interfere destructively between giant resonances and constructively at these resonances so that the results based on the absence of such interferences, in particular the calculation of Sec. V, becomes invalid. We have as yet not found convincing evidence for the viewpoints just put forward.

Finally, it is noted that our formula (28) for M_2 shows no dependence on the energy of the incident particle, although it is found that to explain the data the imaginary part of the complex potential must be increased from about $1\frac{1}{2}$ to 8 Mev as the energy of the incident particle increases from a few to about 20 Mev.[14,15] About one-half of this increase could be accounted for by the increase of the absorption width Γ which appears in the Stieltjes transform (11) (see Appendix B of reference 3).

[20] The polarization of the nucleus by one of the particles contained therein was discussed by K. M. Watson, Phys. Rev. **89**, 575 (1953); N. C. Francis and K. M. Watson, Phys. Rev. **92**, 291 (1953); Brueckner, Levinson, and Mahmoud, Phys. Rev. **95**, 655 (1954); Gyo Takedo and K. M. Watson, Phys. Rev. **97**, 1336 (1955).

PHYSICAL REVIEW VOLUME 98, NUMBER 3 MAY 1, 1955

Gamma Rays from the Inelastic Scattering of Neutrons in Aluminum, Magnesium, and Silver*

L. A. RAYBURN,† D. L. LAFFERTY,‡ AND T. M. HAHN§
Department of Physics, University of Kentucky, Lexington, Kentucky

(Received April 1, 1954)

Monoenergetic neutrons from the $H^2(d,n)He^3$ reaction were used to bombard scatterers each in the form of a ring surrounding an unshielded NaI(Tl) gamma-ray spectrometer. The gamma-ray spectrum for each scatterer was obtained by subtracting the background counting rate from the counting rate with the scatterer in place. An analysis of the gamma-ray spectra yields discrete gamma-rays for each scatterer as follows: Al: 0.422*, 0.843, 0.988, 1.69, and 2.10 Mev; Mg: 0.438, 0.555, 0.688, 0.837, 1.00, 1.34, 1.91, 2.08*, and 2.44 Mev; Ag: 0.332*, 0.696, 0.795, 1.10, 1.99, 2.13*, 2.32, and 2.54* Mev. The starred gamma-ray energies denote those that have not been previously reported.

INTRODUCTION

IN the neutron inelastic scattering process the incident neutron energy is reduced, and the target nucleus is left in an excited state. The excited nucleus generally decays to its ground state by the emission of one or more gamma rays. The nuclear energy levels may be obtained directly from a measurement of the energies of the groups of inelastically scattered neutrons. Very little information[1] has been obtained in this way due to the very poor energy resolution of neutron spectrometers. Energy level separations may be determined by a measurement of the energies of the de-excitation gamma rays. The determination of the energies of the de-excitation gamma rays has been the subject of many investigations.[2–11]

EXPERIMENTAL PROCEDURE

Monoenergetic neutrons with an energy of ~2.7 Mev were obtained from the $H^2(d,n)He^3$ reaction. The deuterons were accelerated in the University of Kentucky 120-kv low-voltage accelerator. A neutron flux

* Sponsored by the Office of Ordnance Research, U. S. Army.
† Now at Argonne National Laboratory, Lemont, Illinois.
‡ Present address: Vanderbilt University, Nashville, Tennessee.
§ Now at Virginia Polytechnic Institute, Blacksburg, Virginia.
[1] Little, Long, and Mandeville, Phys. Rev. **69**, 414 (1946).
[2] Grace, Beghian, Preston, and Halban, Phys. Rev. **82**, 969 (1951).
[3] R. B. Day, Phys. Rev. **89**, 908 (1953).
[4] Scherrer, Smith, Allison, and Faust, Phys. Rev. **91**, 768 (1953).
[5] Scherrer, Theus, and Faust, Phys. Rev. **91**, 1476 (1953).
[6] Garrett, Hereford, and Sloope, Phys. Rev. **92**, 1507 (1953).
[7] L. C. Thompson, Phys. Rev. **89**, 905 (1953).
[8] R. M. Kiehn and C. Goodman, Phys. Rev. **93**, 177 (1954).
[9] M. A. Rothman and C. E. Mandeville, Phys. Rev. **93**, 796 (1954).
[10] Lafferty, Rayburn, and Hahn, Phys. Rev. **96**, 381 (1954).
[11] Rayburn, Lafferty, and Hahn, Phys. Rev. **94**, 1641 (1954).

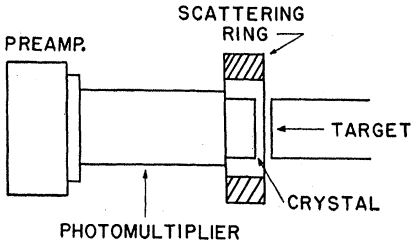

FIG. 1. Experimental arrangement of the neutron source, scatterer, and gamma-ray detector.

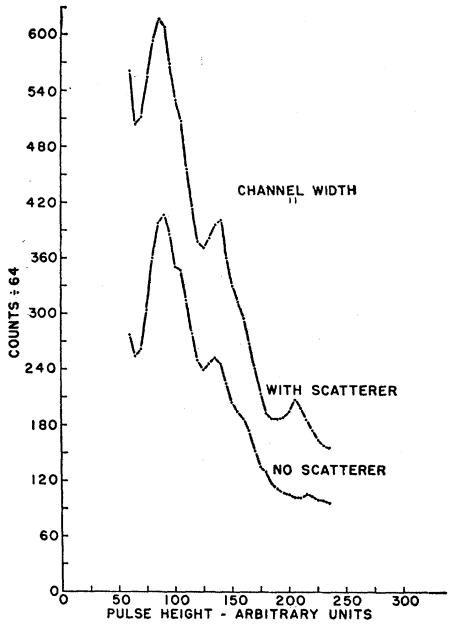

FIG. 2. Gross gamma-ray spectrum with and without the scatterer in place.

of 10^7 neutrons per sec was obtained from 200 μa of deuterons incident on a liquid-cooled deuterated paraffin target deposited on a sheet of 5-mil thick copper. These neutrons were used to bombard scatterers each in the form of a ring surrounding an unshielded NaI(Tl) crystal, which was part of a gamma-ray spectrometer. The neutron flux was monitored by a pair of enriched BF_3 counters. The experimental arrangement is shown in Fig. 1.

The NaI(Tl) crystal was mounted on a DuMont 6292 photomultiplier tube. The pulses from the photomultiplier tube were analyzed with a single-channel differential pulse-height analyzer. The gamma-ray spectrometer was calibrated using the gamma rays from Na^{22} (0.511 Mev) and Cs^{137} (0.661 Mev). The spectrometer had a resolution of 10 percent as measured for the 0.661-Mev gamma ray from Cs^{137}.

The complex gamma-ray spectrum for each scatterer was obtained by subtracting the counting rate with the ring scatterer removed from the counting rate with the scatterer in place. An example of the gross gamma-ray spectrum with and without a scatterer (Cu, in this case) in place is shown in Fig. 2. The large peak in the no-scatterer curve in Fig. 2 is believed due in part to neutron capture in the iodine of the NaI crystal. The radioactive iodine that is produced has a measurable half-life of 25 min. Any contribution of this effect in the subtraction process may be eliminated by exposing the NaI crystal to the neutron flux for a sufficient time (~1 hr) so that secular equilibrium is reached before any usable data are taken.

EXPERIMENTAL RESULTS

In all of the figures showing the gamma-ray spectra for different scatterers, the ordinates have been normalized with respect to the BF_3 monitor counting rate. The counting time is greater for the higher-energy portions of the curves showing the spectrum for each scatterer in detail. In these figures the discrete gamma-rays are identified by their photoelectric peak, *P*; characteristic Compton edge, *C*; and pair peak, *PR*. The figures showing the spectrum for each scatterer plotted to the same scale were obtained from the

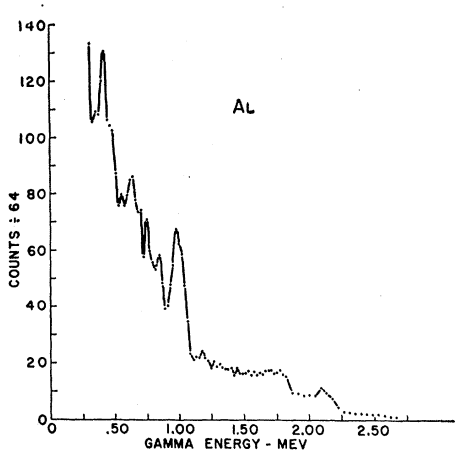

FIG. 3. The gamma-ray spectrum from an aluminum scatterer.

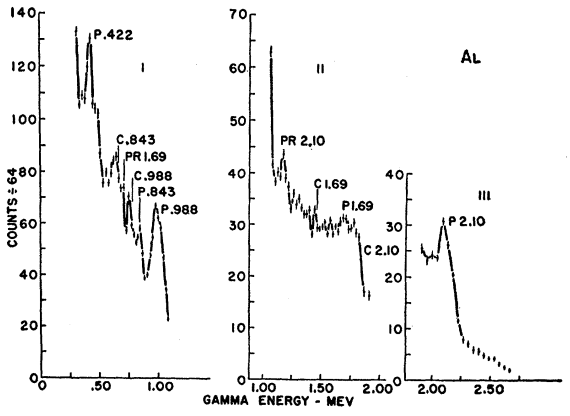

FIG. 4. The gamma-ray spectrum from aluminum shown in greater detail. The channel width in region I was 0.022 Mev and in regions II and III 0.044 Mev.

TABLE I. Comparison of gamma-ray energy values for Al; all energies are in Mev.

Present work	Other energy values							
(1)	(2)[a]	(3)[b]	(4)[c]	(5)[d]	(6)[e]	(7)[f]	(8)[g]	(9)[h]
0.422	···	···	···	···	···	···	···	···
0.843	0.843	···	0.82	···	0.80	0.844	0.84	0.84
0.988	1.018	···	1.02	0.95	0.97	1.016	1.01	1.01
1.69	···	1.7	···	···	···	···	···	···
2.10	2.20	···	2.34	2.14	2.15	2.259	2.23	···

[a] See reference 3.
[b] See reference 5.
[c] See reference 6.
[d] Brolley, Sampson, and Mitchell, Phys. Rev. **76**, 624 (1949).
[e] E. H. Rhoderick, Nature **163**, 848 (1949).
[f] E. M. Reilley *et al.*, Phys. Rev. **86**, 857 (1952).
[g] H. F. Stoddart and H. E. Gove, Phys. Rev. **87**, 262 (1952).
[h] D. M. Van Patter and W. W. Buechner, Phys. Rev. **87**, 51 (1952).

detailed spectra by normalizing all portions to the channel width and counting time of the first portion.

The gamma-ray spectrum obtained by the subtraction process for an aluminum scatterer is shown in Fig. 3. The gamma-ray spectrum from an aluminum scatterer is shown in greater detail in Fig. 4. As shown in Fig. 4, there are discrete gamma-rays with energies of 0.422, 0.843, 0.988, 1.69, and 2.10 Mev. The gamma ray at 0.422 Mev has not been previously reported. It is probable that this gamma ray arises from a transition between the 2.10-Mev and 1.69-Mev excited states. There are contributions to the spectrum from unresolved gamma rays in the vicinity of 1.5 Mev (see Fig. 4). These gamma-ray energies are compared with those of other investigators in Table I.

The gamma-ray energies listed in columns (2), (3), and (4) of Table I were found from neutron inelastic scattering. Those listed in columns (5), (6), (7), and (8) were found from proton inelastic scattering. Those listed in column (9) were determined from the charged particle reaction $Si^{29}(d,\alpha)Al^{27}$.

The gamma-ray spectrum from a scatterer of magnesium is shown in Fig. 5. The large, rather obvious photoelectric peak at 1.34 Mev is the only reported gamma ray seen in previous neutron inelastic scattering experiments.

The gamma-ray spectrum from a magnesium scatterer is shown in greater detail in Fig. 6. An analysis of this spectrum yields discrete gamma rays with energies of 0.438, 0.555, 0.688, 0.837, 1.00, 1.34, 1.91, 2.08, and 2.44 Mev. The gamma-ray at 2.08 Mev has not been previously reported. In Fig. 6 it is seen that the shape of the Compton distribution for the 2.44-Mev gamma ray has been somewhat altered by the 2.08-Mev photoelectric peak. The pair peak for the 2.44-Mev gamma ray falls under the 1.34-Mev photoelectric peak and consequently cannot be seen. The pair peak of the 2.08-Mev gamma ray falls under the Compton peak of the 1.34-Mev gamma ray. The pair peak for the 1.34-Mev gamma ray is only partly seen at the extreme low-energy end of the spectrum. The Compton peak for the 1.00-Mev gamma ray is partially

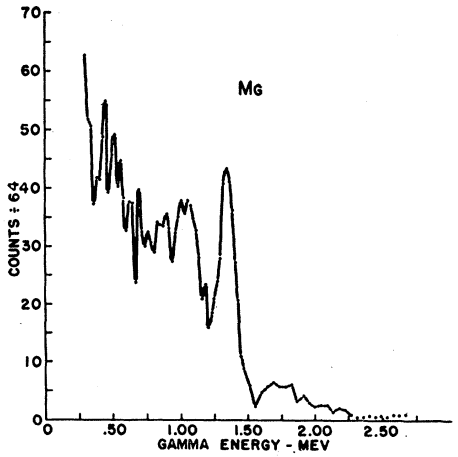

FIG. 5. The gamma-ray spectrum from a amgnesium scatterer.

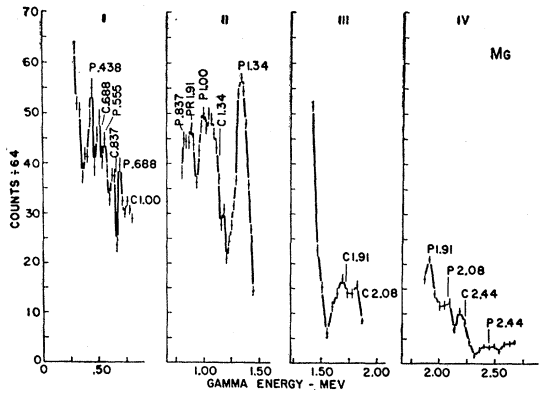

FIG. 6. The gamma-ray spectrum from a magnesium scatterer shown in greater detail. The channel width in region I was 0.022 Mev and in regions II, III, and IV, 0.044 Mev.

obscured by the 0.837- and 0.688-Mev photoelectric peaks. The Compton peak for the 0.555-Mev gamma ray cannot be seen as such since the 0.438-Mev photoelectric peak falls on top of it.

TABLE II. Comparison of gamma-ray energy values for Mg; all energies are in Mev.

Present work	Other energy values						
(1)	(2)[a]	(3)[b]	(4)[c]	(5)[d]	(6)[e]	(7)[f]	(8)[g]
0.438	···	···	···	···	···	···	0.41
0.555	···	···	···	···	0.57	0.583	···
0.688	···	···	···	···	···	···	0.63
0.837	···	···	···	···	···	···	0.80
1.00	···	···	···	1.00	0.96	0.976	···
1.34	1.365	1.4	1.32	1.33	···	···	1.38
···	···	···	···	1.56	1.63	1.611	···
1.91	···	···	···	1.98	1.97	1.957	···
2.08	···	···	···	···	···	···	···
2.44	···	···	···	2.64	···	2.562	···

[a] See reference 3.
[b] See reference 6.
[c] R. H. Dicke and J. Marshall, Jr., Phys. Rev. **63**, 86 (1943).
[d] H. W. Fulbright and R. R. Bush, Phys. Rev. **74**, 1323 (1948).
[e] Schelberg, Sampson, and Cochran, Phys. Rev. **80**, 574 (1950).
[f] P. M. Endt *et al.*, Phys. Rev. **87**, 27 (1952).
[g] O. H. Turner, Australian J. Phys. **6**, 380 (1953).

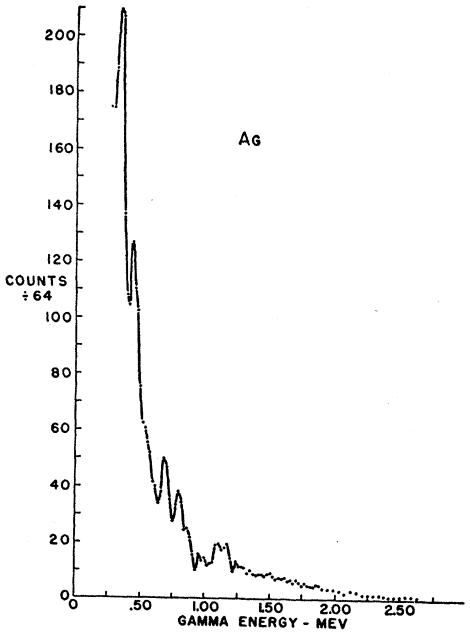

FIG. 7. The gamma-ray spectrum from a silver scatterer.

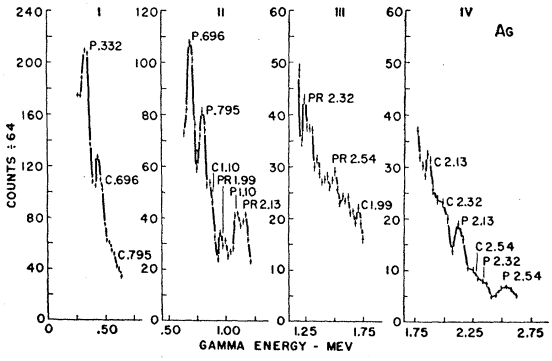

FIG. 8. The gamma-ray spectrum from a silver scatterer shown in greater detail. The channel width in region I was 0.022 Mev and in regions II, III, and IV, 0.044 Mev.

The gamma-ray energies reported here are compared with those of other investigators in Table II. The energies listed in columns (2) and (3) in Table II are from neutron inelastic scattering. Those listed in columns (4) and (5) are from proton inelastic scattering. Those listed in column (6) are from the $Al^{27}(d,\alpha)Mg^{25}$ reaction. Those listed in column (7) are from the $Al^{27}(d,\alpha)Mg^{25}$ and $Mg^{24}(d,p)Mg^{25}$ reactions. Those listed in column (8) are from the $Na^{23}(p,\gamma)Mg^{24}$ reaction. In Fig. 6 some evidence of an unresolved gamma ray is seen at ~1.5 Mev; this probably corresponds to the 1.6-Mev gamma ray reported by other workers (see Table II).

The gamma-ray spectrum from a scatterer of silver is shown in Fig. 7. The spectrum for silver is shown in greater detail in Fig. 8. An analysis of the spectrum yields discrete gamma-rays with energies of 0.332, 0.696, 0.795, 1.10, 1.99, 2.13, 2.32, and 2.54 Mev. It is seen in Fig. 8 that the 1.99-Mev photoelectric peak was not resolved; however, the Compton edge and pair peak are easily seen. The 2.32-Mev photoelectric peak was only partially resolved. These energy assignments are compared with those of other investigators in Table III.

The gamma rays at 0.332, 2.13, and 2.54 Mev have not been previously reported. There is an indication of some unresolved peaks at approximately 1.6 Mev in Fig. 8. It is probable that this corresponds to the 1.5-Mev gamma ray reported by other workers (see Table III). In Table III the energies listed in column (2) were obtained from neutron inelastic scattering, those in column (3) from the decay of 6.7-hr $Cd^{107,109}$, and those in column (4) from nuclear excitation by high-energy x-rays.

TABLE III. Comparison of gamma-ray energy values for Ag; all energies are in Mev.

Present work (1)	Other energy values (2)[a]	(3)[b]	(4)[c]
0.332	...	...	...
0.696	0.63	...	...
0.795	...	0.846	...
1.10	1.1	...	...
...	1.5	...	1.59
1.99	...	...	1.95
2.13	...	...	...
2.32	...	...	2.32
2.54	...	...	...

[a] See reference 4.
[b] H. Bradt *et al.*, Helv. Phys. Acta **18**, 351 (1945).
[c] M. L. Wiedenbeck, Phys. Rev. **67**, 59 (1945).

Note added in proof.—Due to the difficulty in properly displaying such complex spectra it is felt that some further remarks would be helpful. It was recognized that since the background was relatively large, small fluctuations in it or in the response of the detecting equipment would cause erroneous results. For this reason several independent spectra, with and without the scatterer in position, were obtained for each scatterer. The difference curves for these independent determinations showed no significant differences. The mean of these independent determinations is what is shown for each scatterer. In order to use the experimental procedure the contribution to the background by neutrons scattered into the detector by the scattering sample must be small. It was estimated from the size of the scattering samples used, their neutron cross sections, and the geometry that this contribution would be small. This estimate has been confirmed by the use of a carbon scatterer in the background determination (see reference 10).